

Kinetics and Mechanism for CO₂ Scrambling in a N-Carboxyimidazolidone Analogue for N¹-Carboxybiotin

Fiona J. Lihs and M. Tyler Caudle*

Contribution from the Department of Chemistry and Biochemistry, Arizona State University, Tempe, Arizona 85287-1604

Received May 1, 2002

Abstract: The N-carboxyimidazolidone anion, **2**⁻, was prepared as an analogue for N¹-carboxybiotin, and the kinetics of its CO₂-dependent chemistry were studied in polar aprotic media. The objective was to assess the viability of unimolecular CO₂ elimination from N¹-carboxybiotin as a microscopic step in biotin-dependent carboxyl transfer enzymes. The anionic **2**⁻ was prepared as its lithium salt by first deprotonating 2-imidazolidone with phenyllithium, followed by direct reaction with carbon dioxide. This procedure also permitted isolation of the ¹³C enriched derivative **2**⁻{¹³C} by reaction with ¹³CO₂. Proton and ¹³C NMR and isotope-dependent FTIR measurements confirmed that carboxylation had occurred at the nitrogen atom of 2-imidazolidone to give **2**⁻. Time-dependent FTIR spectroscopy showed that Li**2** undergoes carboxyl exchange with free carbon dioxide, with kinetics indicative of rate-limiting unimolecular dissociation of the N-CO₂ bond. Under these conditions, the weak Lewis acid Mg²⁺ catalyses the exchange of **2**⁻ with free CO₂, which appears to be related to the ability of the metal ion to coordinate to **2**⁻. Reaction of Li**2** with carboxylic acids in DMSO results in acid-dependent decarboxylation of **2**⁻ with a rate that is dependent on the concentration of the acid and its pK_a. A common mechanistic framework is presented for both Lewis acid catalyzed carboxyl exchange and acid-dependent decarboxylation that involves initial interaction at the carbonyl oxygen and which has the effect of polarizing the nitrogen lone pair toward the imidazolidone ring rather than the carboxyl group. Lewis acid interaction with the carbonyl oxygen thus weakens the N-CO₂⁻ bond and functions as a trigger for dissociation of CO₂. In the context of biotin-dependent enzymes, this suggests a means by which the kinetically stable N¹-carboxybiotin cofactor intermediate might be triggered for dissociation of CO₂.

Introduction

Biotin is the critical organic cofactor in biotin-dependent carboxyl transfer enzymes (BDCs), which are important in mammalian and avian fatty acid biosynthesis.¹⁻³ Biotin, when covalently bound to the BDC enzyme complex, functions to shuttle a carboxyl group between two independent enzyme active sites. In the first active site, called biotin carboxylase, the biotin cofactor is carboxylated at the N¹ position by accepting a carboxyl group from bicarbonate. The functionalized N¹-carboxybiotin is then translocated to the second active site, called carboxyl transferase, where it transfers the carboxyl group to a terminal acyl substrate. This latter reaction has been postulated to occur via initial elimination of CO₂ from N¹-carboxybiotin in the carboxyl transferase active site,^{2,3} Scheme 1, but there is presently no chemical basis for this hypothesis. Thus, the gross mechanistic features of this enzymatic process have been characterized, but many chemical details of N¹-carboxybiotin formation, translocation, and decarboxylation in BDC enzymes are still unresolved.

The fundamental chemistry of BDC enzymes is of interest since these enzymes affect a net transfer of carbon dioxide from

a CO₂-equivalent, bicarbonate, to a carbon nucleophile, forming a new carbon-carbon bond in the process. As a consequence, model studies have sought to mimic fundamental chemical steps believed to occur in the enzyme.⁴⁻⁶ Many of these have centered on 2-imidazolidone, **1**, and related derivatives as a model for the biotin headgroup. The general consensus arising from these chemical studies is (1) that biotin itself is a poor nucleophile and requires preactivation, probably by proton transfer,⁷ in order to accept the carboxyl group and (2) that N¹-carboxybiotin is a kinetically poor carboxyl donor and probably requires enzymatic

- (4) Kluger, R. A.; Tsao, B. *J. Am. Chem. Soc.* **1993**, *115*, 2089-2090. Musashi, Y.; Hamada, T.; Sakaki, S. *J. Am. Chem. Soc.* **1995**, *117*, 11320-11326. Cravey, M. J.; Kohn, H. *J. Am. Chem. Soc.* **1980**, *102*, 3928-3939. Kohn, H. *J. Am. Chem. Soc.* **1976**, *98*, 3690-3694. Kondo, H.; Miura, K.; Sunamoto, J. *Tetrahedron Lett.* **1982**, *23*, 659-662. Botella, J. M.; Klabebe, A.; Perie, J.; Monnier, E. *Tetrahedron* **1992**, *48*, 5111-5122. Caplow, M. *J. Am. Chem. Soc.* **1965**, *87*, 5774-5785. Bruice, T. C.; Hegarty, A. F. *Proc. Natl. Acad. Sci. U.S.A.* **1970**, *65*, 805-809.
- (5) Caplow, M.; Yager, M. *J. Am. Chem. Soc.* **1967**, *89*, 4513-4521.
- (6) Mori, H.; Makino, Y.; Yamamoto, H.; Kwan, T. *Chem. Pharm. Bull.* **1973**, *21*, 915-916. Otsuji, Y.; Arakawa, M.; Matsumura, N.; Haruki, E. *Chem. Lett.* **1973**, 1193-1196. Sakurai, H.; Shirahata, A.; Hosomi, A. *Tetrahedron Lett.* **1980**, *221*, 1967-1970. Matsumura, N.; Asai, N.; Yoneda, S. *J. Chem. Soc., Chem. Commun.* **1983**, 1487-1488.
- (7) Attwood, P. V.; Tipton, P. A.; Cleland, W. W. *Biochemistry* **1986**, *25*, 8197-8205. Tipton, P. A.; Cleland, W. W. *Biochemistry* **1988**, *27*, 4317-4325. Fry, D. C.; Fox, T. L.; Lane, M. D.; Mildvan, A. S. *J. Am. Chem. Soc.* **1985**, *107*, 7659-7665. Perrin, C. L.; Dwyer, T. J. *J. Am. Chem. Soc.* **1987**, *109*, 5163-5167. Levert, K. L.; Lloyd, R. B.; Waldrop, G. L. *Biochemistry* **2000**, *39*, 4122-4128.

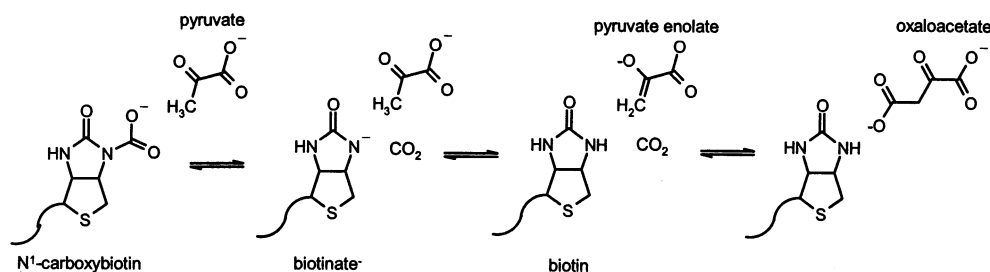
To whom correspondence should be addressed. E-mail: tcaudle@asu.edu.

(1) Jitrapakdee, S.; Wallace, J. C. *Biochem. J.* **1999**, *340*, 1-16.

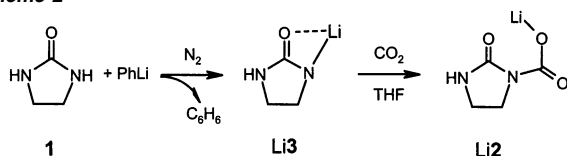
(2) Knowles, J. R. *Annu. Rev. Biochem.* **1989**, *58*, 195-221.

(3) Attwood, P. V.; Wallace, J. C. *Acc. Chem. Res.* **2002**, *35*, 113-120.

Scheme 1



Scheme 2



activation to facilitate N–CO₂ bond cleavage. It is therefore important to understand factors affecting the reactivity of *N*¹-carboxybiotin, which may be relevant to its enzymatic catalysis.

The aqueous chemistry of *N*¹-carboxybiotin decarboxylation shows a dependence on pH indicative of both acid-dependent and acid-independent pathways.⁸ We have sought to characterize these pathways in nonaqueous media for several reasons. First, nonaqueous solvents have been shown to increase the rate for decarboxylation of *N*-carboxylimidazolidone, suggesting desolvation of *N*¹-carboxybiotin may play a role in carboxyl transfer.⁹ Second, Lewis acid interactions with the carboxylimidazolidone functional group, including proton transfer and metal binding, can be more directly controlled in aprotic media, enabling more detailed study of these interactions.

In this paper, we report on the preparation of *N*-carboxylimidazolidone, **2**[−], directly from 2-imidazolidone, **1**, Scheme 2, using carbon dioxide as the CO₂ source. This molecule is a direct analogue for the headgroup of the *N*¹-carboxybiotin intermediate in BDC enzymes. We show that **2**[−] undergoes carboxyl exchange with free CO₂ and that the kinetics of this reaction clearly indicate rate-limiting N–CO₂ bond cleavage. Compound **2**[−] can be protonated by enzymatically relevant Brønsted acids resulting in the decarboxylation of **Li2** two orders of magnitude more rapidly than carboxyl exchange on **2**[−]. Catalysis of carboxyl exchange by the weak Lewis acid Mg²⁺ is also examined as a general model for noncovalent interactions with *N*¹-carboxybiotin that may be important in CO₂ transfer by BDC enzymes.

Experimental Section

Materials. Phenyllithium as a 2 M solution in cyclohexane and ether was obtained from Acros. The 2-imidazolidone precursor was obtained from Aldrich, recrystallized from tetrahydrofuran (THF), and stored under nitrogen. THF was distilled from sodium benzophenone ketyl and stored under nitrogen. Dimethyl sulfoxide (DMSO) and DMSO-*d*₆ were vacuum-distilled from calcium hydride and stored under nitrogen. ¹³CO₂ gas (99%) was obtained from Cambridge Isotope Laboratories. All preparative and analytical manipulations were carried out under nitrogen either in a nitrogen-filled glovebox or using standard Schlenk apparatus.

Lithium *N*-Carboxy-2-imidazolidone. (**Li2**) 1.0 g (11.6 mmol) 2-imidazolidone, **1**, was suspended in 50 mL anhydrous THF. One equivalent of 2.0 M phenyllithium solution (5.8 mL, 11.6 mmol) was added dropwise while stirring. Once all of the phenyllithium had been added, the reaction was stirred under one atm of dry CO₂ gas for 12 h. The resulting white precipitate was collected by filtration using Schlenk techniques. IR (KBr, cm^{−1}) 1716, 1633, 1340, 1255, 1172, 810, 730. ¹H NMR (DMSO, ppm) δ 3.16(triplet), 3.6(triplet), 6.1(singlet). The ¹H NMR spectrum also shows the presence of unreacted **1** and about 1 equiv water associated with **Li2** in the product. Analysis found (calc)% for (Li₂)(I)_{0.14}(H₂O)_{1.1}: C, 31.1(31.6); H, 4.2(4.8); N, 18.7(19.0).

Lithium *N*-¹³C}Carboxy-2-imidazolidone. (**Li2**{¹³C}) 0.10 g (1.16 mmol) 2-imidazolidone, **1**, was suspended in 10 mL anhydrous THF. One equivalent of 2.0 M phenyllithium solution (0.58 mL, 1.16 mmol) was added dropwise while stirring. Once all of the phenyllithium had been added, the reaction was stirred under one atm dry ¹³CO₂ gas for 10 min. The resulting white precipitate was collected by filtration using Schlenk techniques. For **Li2**{¹³C}: ¹H NMR (DMSO, ppm) δ 3.16, 3.6, 6.1 IR (KBr, cm^{−1}) 1716, 1600, 1340, 1255, 1172, 805, 730.

CO₂ Exchange Kinetics. Kinetics were measured using a two-syringe rapid mixing apparatus connected to an infrared-transparent flow cell with ZnS windows. The flow cell was mounted inside a Nicolet Avatar 360 Fourier transform infrared spectrometer. Reaction was initiated when the two reagent solutions were rapidly mixed and directed into the flow cell. The time-dependent infrared spectrum was monitored between 2380 and 2230 cm^{−1}, the CO₂ region of the spectrum. Kinetic decay curves were extracted from the time-dependent spectra and fit to a first-order exponential decay to derive the observed rate constant, *k*_{obs}.

A sealed gas control apparatus was used to prepare a solution of DMSO preequilibrated with approximately 760 mmHg of ¹³CO₂, which equates to 0.130 M CO₂ in solution.¹⁰ This solution served as a stock solution for the preparation of reagent solutions of varying concentrations of ¹³CO₂. The desired reagent solution was mixed with a solution of **2**[−] and delivered to the IR cell using the apparatus described above. The same procedure was used for the magnesium-dependent experiment, except that the solution of **2**[−] was premixed with varying concentrations of Mg²⁺. For decarboxylation kinetic experiments, the sample of **2**[−] in DMSO was reacted with the appropriate carboxylic acid and the time-dependent IR spectrum in the CO₂ region was monitored. In this case, only the formation of free ¹²CO₂ in solution was observed.

Results

The reaction of lithium imidazolidonate, **Li3**, with gaseous carbon dioxide in THF results in precipitation of a white solid, **Li2**, Scheme 2, which evolves carbon dioxide upon treatment with strong acid. CHN and ¹H and ¹³C NMR spectroscopy suggested that the isolated product is an approximately 88:12 mixture of **Li2** and unreacted **1**, which could not be separated.

(8) Tipton, P. A.; Cleland, W. W. *J. Am. Chem. Soc.* **1988**, *110*, 5866–5869.

(9) Rahil, J.; You, S.; Kluger, R. *J. Am. Chem. Soc.* **1996**, *118*, 12495–12498.

Gao, D.; Pan, Y.-K. *J. Org. Chem.* **1999**, *64*, 1151–1159.

(10) Welford, P. J.; Brookes, B. A.; Wadhawan, J. D.; McPeak, H. B.; Hahn, C. E. W.; Compton, R. G. *J. Phys. Chem. B* **2001**, *105*, 5253–5261.
Gennaro, A.; Isse, A. A.; Vianello, E. *J. Electroanal. Chem. Interfacial Electrochem.* **1990**, *289*, 203–215.

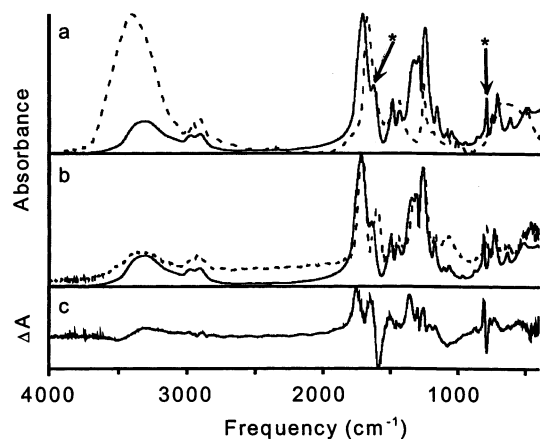


Figure 1. (a) Infrared spectra of **1** (dashed) and **2** (solid), showing appearance of the $-\text{CO}_2$ bands (*) at 1633 and 810 cm^{-1} . (b) Infrared spectra of Li_2 (solid) and $\text{Li}_2\{^{13}\text{C}\}$ (dashed) showing shifts in the $^{13}\text{CO}_2$ sensitive bands. (c) Difference spectrum ($\text{Li}_2 - \text{Li}_2\{^{13}\text{C}\}$). Infrared spectra were measured in the solid state as KBR pellets.

Washing with hot THF reduced the amount of **1** somewhat but did not result in a homogeneous sample of Li_2 . The infrared spectrum of the product shows formation of two important new bands at 1625 and 803 cm^{-1} that are absent in **1**, Figure 1a. These are characteristic of the asymmetric stretching and scissoring modes, respectively, of the $-\text{CO}_2^-$ moiety in $\mathbf{2}^-$. In the spectrum of $\mathbf{2}\{^{13}\text{C}\}$ prepared from $^{13}\text{CO}_2$, these modes shift to lower energy as demonstrated in Figure 1b and c, confirming that the carboxyl group arises from CO_2 gas and that the IR assignments are correct. The carbonyl band at 1700 cm^{-1} remains nearly unchanged by isotope labeling at the carboxyl carbon, demonstrating the carboxylation does not directly involve the carbonyl group but rather occurs at the nitrogen center. These isotope-dependent vibrational assignments are consistent with those made by Clarkson and Carey.¹¹

The proton NMR spectrum of Li_2 in $\text{DMSO}-d_6$, Figure 2, also demonstrates carboxylation at the nitrogen center. The triplet signals from $\mathbf{2}^-$ at 3.16 and 3.60 ppm show that the methylene protons are inequivalent on the NMR time scale, but are equivalent in **1**. We also see a new resonance at 6.85 ppm that is not present in **1** and that integrates to a single proton when compared with the ethylene signals of $\mathbf{2}^-$, and which we assign to the $-\text{NH}$ proton of $\mathbf{2}^-$. There is no evidence from either NMR data or from compositional analysis for the formation of any dicarboxylated complex. We therefore formulate Li_2 as shown in Scheme 2.

At the limit of solubility in DMSO , the ^{13}C NMR signal arising from the carbamate carbon in unenriched Li_2 is not observable. However, when the solution is exposed to $^{13}\text{CO}_2$ gas, a ^{13}C NMR signal at 152 ppm is clearly observed, Figure 3. This indicates that the carboxyl group in Li_2 is exchanged with free $^{13}\text{CO}_2$ on this time scale, resulting in enrichment of the carboxyl carbon in ^{13}C . Time-dependent NMR spectra showed that this reaction was complete within about 30–60 min, making ^{13}C NMR unsuitable for measurement of rate data since each ^{13}C NMR spectrum took at least 6 min to collect. Furthermore, the NMR experiment does not distinguish a carboxyl exchange process from a simple $^{13}\text{CO}_2$ absorption process since we cannot directly observe formation of $^{12}\text{CO}_2$.

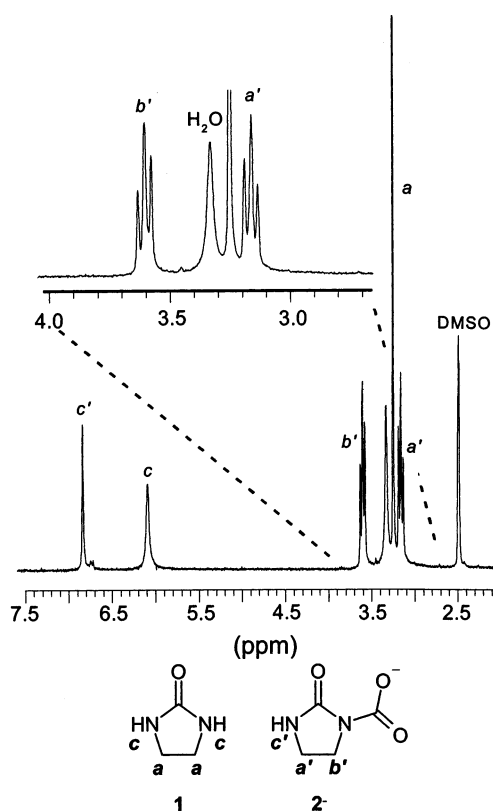


Figure 2. 300 MHz ^1H NMR spectrum of Li_2 in $\text{DMSO}-d_6$.

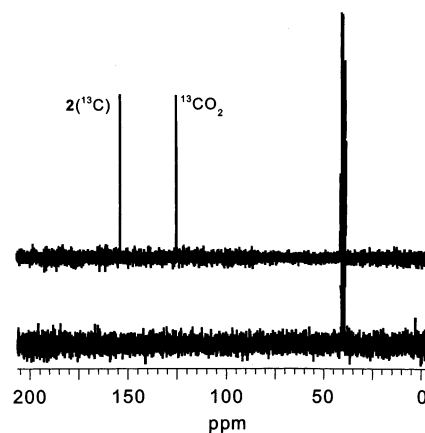


Figure 3. ^{13}C NMR spectra of Li_2 in $\text{DMSO}-d_6$ containing natural abundance ^{13}C (bottom) and after exposure to $^{13}\text{CO}_2$ (top).

To address this problem, we used Fourier transform infrared spectroscopy to track the $^{12}\text{CO}_2/^{13}\text{CO}_2$ exchange. This technique took advantage of the fact that $^{12}\text{CO}_2$ and $^{13}\text{CO}_2$ exhibit separate infrared bands at 2337 and 2271 cm^{-1} , respectively, which are both within the IR solvent window of DMSO . For $^{13}\text{CO}_2$ absorption, we should observe a simple decrease in the intensity of the free $^{13}\text{CO}_2$ band whereas for carboxyl exchange, loss of free $^{13}\text{CO}_2$ will be accompanied by a concomitant increase in $^{12}\text{CO}_2$. FTIR had the additional advantage of permitting us to collect real-time data on the 1-h time scale, so we were able to obtain kinetic information about the reaction as well.

When a solution of Li_2 is rapidly mixed with a solution containing dissolved $^{13}\text{CO}_2$, the time-dependent FTIR spectra in Figure 4 are obtained. These data show a decrease in the intensity of the $^{13}\text{CO}_2$ band at 2271 cm^{-1} and a concomitant increase in the $^{12}\text{CO}_2$ band at 2337 cm^{-1} . When the intensity at

(11) Clarkson, J.; Carey, P. R. *J. Phys. Chem.* **1999**, *103*, 2851–2856.

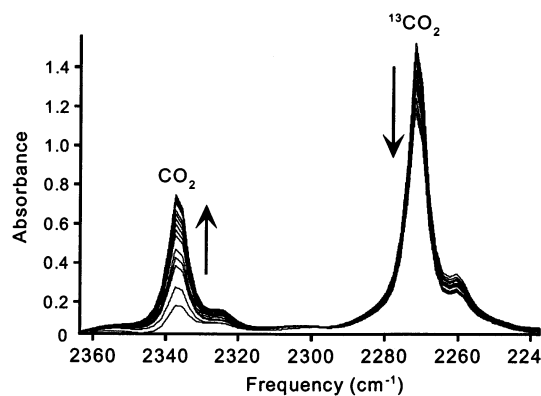


Figure 4. Time-dependent FTIR spectra in the free CO₂ region upon mixing Li2 with ¹³CO₂ in DMSO. The arrows show decrease in absorbance at 2271 cm⁻¹ (¹³CO₂) and increase in absorbance at 2337 cm⁻¹ (¹²CO₂) with time.

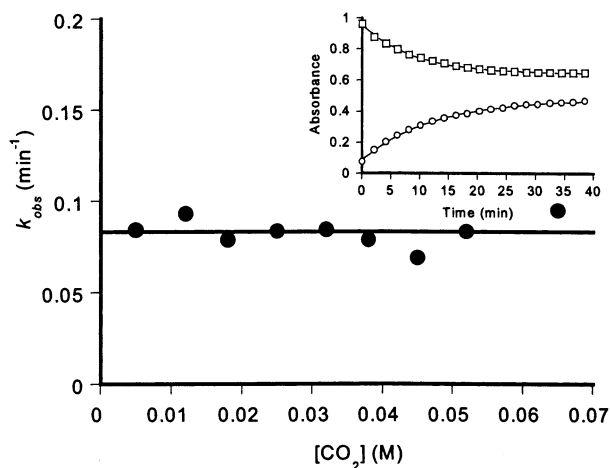


Figure 5. Observed first-order rate constants k_{obs} for carboxyl exchange by Li2 in DMSO as a function of total [CO₂]. The solid line shows a linear fit to the data, giving $k_{\text{obs}} = 0.083(5) \text{ min}^{-1} + 0.0 \text{ M}^{-1} \text{ min}^{-1} [\text{CO}_2]$. [Li2] = 0.040 M, $T = 25^\circ\text{C}$. (inset) Decay curves showing time-dependent decrease at 2271 cm⁻¹ (□) and increase at 2337 cm⁻¹ (○). Solid lines are fit to the equation $(A - A_\infty) = (A_0 - A_\infty)e^{-k_{\text{obs}}t}$ to obtain k_{obs} .

these two wavelengths is plotted against time, the decay curves in Figure 5(inset) are obtained. The decrease in intensity at 2271 cm⁻¹ is mirrored by the increase at 2337 cm⁻¹. When the data are modeled as a first-order exponential decay, an excellent fit to the experimental data is obtained and essentially identical observed rate constants, k_{obs} , are obtained for loss of free ¹³CO₂ and gain of ¹²CO₂. These data taken together confirm that we are observing a CO₂ exchange process in which the carboxyl group in **2**⁻ is scrambled with free dissolved CO₂. The time scale for equilibration of the system measured by FTIR is consistent with the NMR data in showing that the reaction is complete in about 1 h.

Using the gas transfer device described in the Experimental Section, we prepared reagent solutions of varying concentration of dissolved ¹³CO₂, which were used in studying the dependence of k_{obs} on total CO₂ concentration, [CO₂]₀. These experiments showed that the time-dependent loss of ¹³CO₂ or gain in ¹²CO₂ consistently fit a first-order exponential decay over the range $0 < [\text{CO}_2]_0 < 0.065 \text{ M}$. Moreover, when k_{obs} was correlated with total [CO₂]₀, Figure 5, we found that the reaction is zero order in [CO₂]₀. Fitting a straight line to the data in Figure 5 gave a y-intercept of $0.083(5) \text{ min}^{-1}$ and a slope that is essentially equal

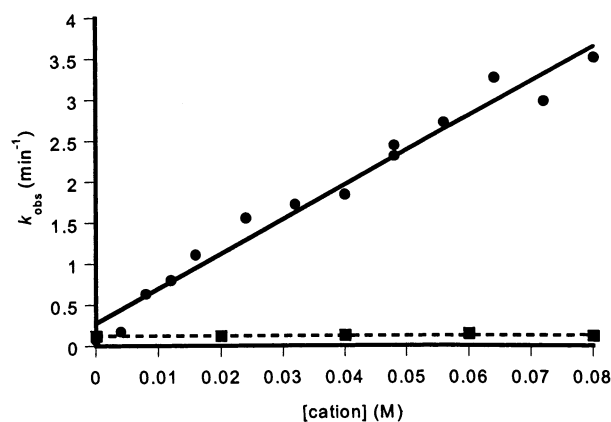


Figure 6. Observed first-order rate constant for CO₂ exchange as a function of [Mg²⁺], (●), and [TBA⁺], (■). Both cations were added as their triflate salts. Solid line shows fit to $k_{\text{obs}} = 2k'K[\text{Mg}^{2+}]_0$. [Li2] = 0.04 M, [CO₂] = 0.035 M, $T = 25^\circ\text{C}$.

to zero. The CO₂ scrambling reaction is first-order in [**2**⁻] and zero-order in [CO₂]. Because NMR spectra show the presence of uncarboxylated **1** in DMSO solutions of **2**⁻, the dependence of the CO₂ scrambling rate on the presence of excess **1** was measured. When one or two additional equivalents of excess **1** were added to the reaction mixture, the rate of carboxyl exchange was unchanged. This shows that the rate is independent of the presence of **1**, consistent with the general observation that there is no direct reaction between **1** and CO₂.

The counteraction affects the CO₂ exchange rate as shown by measuring the carboxyl exchange rates in the presence of Mg(OTf)₂ (OTf⁻ = trifluoromethanesulfonate = triflate) and tetrabutylammonium triflate. For [Mg²⁺] between zero and 0.10 M, we find that the carboxyl exchange rate is increased linearly as [Mg²⁺] increases, Figure 6. This clearly results from the addition of the Mg²⁺ cation since the tetrabutylammonium triflate salt had no effect on the CO₂ exchange rate. Magnesium-catalyzed CO₂ exchange is also independent of the concentration of CO₂ as expected. The exchange reaction was also carried out in the presence of Mg(OTf)₂ and an excess amount of TBA(OTf). These catalyzed rates remained unchanged compared with those containing only Mg(OTf)₂, except at very high concentrations of OTf⁻, which slightly inhibited magnesium catalysis. Our interpretation of this result is that the Mg²⁺ catalysis requires that **2**⁻ bind to it and that the inhibitory effect of high concentrations of triflate is a result of competition for the Mg²⁺. This hypothesis is also consistent with the observation that polydentate magnesium chelators such as 15-crown-5 (1,4,7,10,13-pentaoxacyclopentadecane) also inhibit catalysis of carboxyl exchange by the magnesium ion. A substantial aging effect in these experiments was also observed. When the carboxyl scrambling rate was measured immediately after mixing Li2 with Mg²⁺, the reaction was rapid. However, if samples of Li2 and Mg²⁺ were permitted to age longer than thirty minutes before kinetic measurements, no catalytic effect was observed. This suggests a magnesium-dependent aggregation reaction of **2**⁻ in solution that yields a product inert to carboxyl exchange. Hence all magnesium-dependent kinetics were measured immediately after mixing Li2 and Mg²⁺.

The kinetics for scrambling of the carboxyl group in **2**⁻ with free CO₂ suggests a unimolecular pathway for decarboxylation

Scheme 3

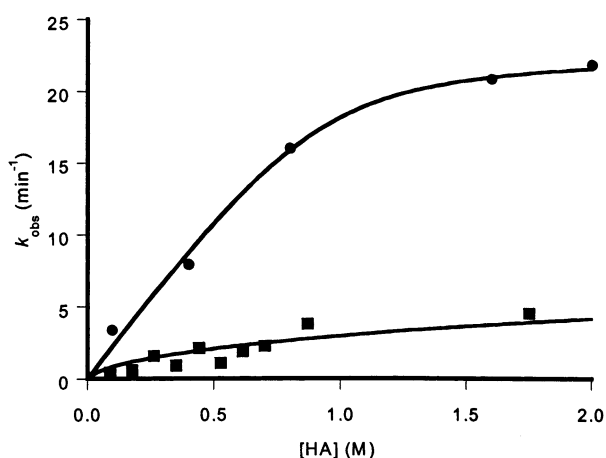
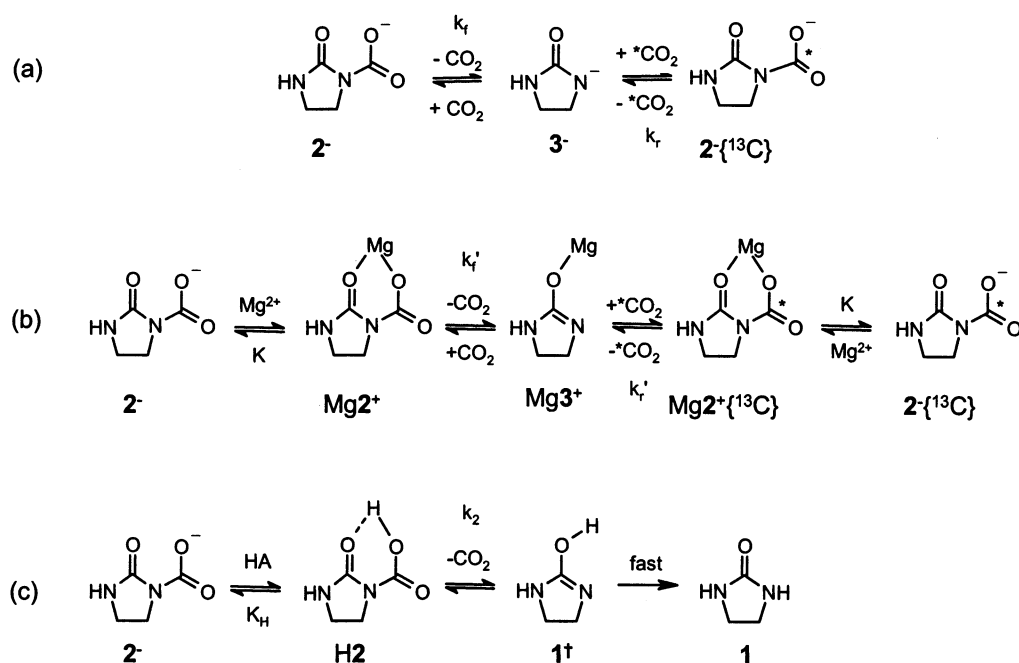


Figure 7. Observed first-order rate constant for decarboxylation of Li2 in DMSO as a function of acid concentration for benzoic acid (●) and acetic acid (■). Solid lines show fits to eq 5. [Li2] = 0.040 M, $T = 25\text{ }^{\circ}\text{C}$.

of 2^- in aprotic media. On the basis of this, we predicted that decarboxylation of 2^- by acids should be independent of the acid concentration and should occur at a rate similar to that for carboxyl exchange. To probe this mechanistic issue, acid-promoted decarboxylation of Li2 by acetic and benzoic acid was studied. Rapidly mixing a DMSO solution of Li2 with a solution of either acid produces CO_2 , whose formation was monitored by FTIR. The time-dependent absorption increase at 2337 cm^{-1} exhibits a first-order exponential rise, indicating that the reaction is first-order in Li2. However, the first-order rate constant is acid-dependent, Figure 7, and increases as the concentration of acid is increased. Decarboxylation of 2^- by benzoic is rapid and exhibits saturation behavior. The acetic acid promoted decarboxylation is slower and exhibits a nearly linear dependence on [HA], consistent with the higher $\text{p}K_{\text{a}}$ of acetic acid. Both of these observations are inconsistent with simple acid-independent decarboxylation followed by protonation of the ureido anion and instead suggests that protonation occurs prior to C–N bond cleavage. The rapid loss of CO_2 upon

protonation is then to be expected since the free carbamic acid H2 is unstable with respect to decarboxylation and rapidly loses CO_2 to give **1**. The observation that carboxyl transfer is catalyzed by Mg^{2+} and that the decarboxylation rate is proton-dependent for 2^- in aprotic media suggests that a common mechanistic framework may be operative in both reactions and that this might be important in the carboxyl transfer reactions catalyzed by biotin enzymes.

Discussion

The mechanism for uncatalyzed carboxyl exchange on 2^- must be consistent with the kinetics that shows that the observed first-order rate constant is independent of $[\text{CO}_2]$. CO_2 scrambling therefore proceeds via a pathway in which the entering CO_2 molecule inserts after the rate-limiting step. This precludes any mechanism involving a dicarboxylated intermediate or a concerted interchange pathway. The kinetic data is therefore most consistent with a rate-determining step involving a unimolecular dissociation of 2^- , generating free CO_2 and the ureido anion 3^- as steady-state intermediates, as shown Scheme 3a. This pathway leads to carboxyl scrambling because reaction of 3^- occurs with either $^{12}\text{CO}_2$ or $^{13}\text{CO}_2$ to regenerate 2^- or give $2^{-}\{^{13}\text{C}\}$. Analysis of Scheme 3a yields the basic rate expression in eq 1.

$$\frac{d[\text{CO}_2]}{dt} = k_f([2^-]_0 - [\text{CO}_2]) - k_r[\text{CO}_2] \quad (1)$$

Neglecting the small ^{13}C isotope effect, we can assume that $k_f = k_r$, which gives eq 2.

$$\frac{d[\text{CO}_2]}{dt} = k_f[2^-]_0 - 2k_f[\text{CO}_2] \quad (2)$$

Equation 2 is a linear inhomogeneous differential equation which yields a first-order exponential decay as its solution with $k_{\text{obs}} = 2k_f$. Scheme 3a therefore gives a rate law consistent with the observed $[\text{CO}_2]$ -independence of k_{obs} . The average value for k_{obs}

over all of the studied CO₂ concentrations is 0.083(2) min⁻¹ so that eq 2 gives a first-order rate constant for cleavage of the C–N bond of $k_f = 0.041(2)$ min⁻¹.

Unimolecular dissociation of free CO₂ from *N*¹-carboxybiotin has been suggested as a critical step in carboxyl transfer in biotin enzymes.^{2,3,8} This has the consequence of generating the highly basic biotinate anion, which is analogous to **3**⁻. The biotinate anion could then function as the base for generating the carbanionic substrate intermediate, leading to a mechanism for CO₂ transfer as shown in Scheme 1. This would be consistent with the work of Stubbe et al. showing that loss of F⁻ from the substrate analogue β-fluoropropionyl-CoA is catalyzed by propionyl-CoA carboxylase, but only under conditions where *N*¹-carboxybiotin is generated by the biotin carboxylase.¹² It has also been shown that biotin-dependent transcarboxylase catalyzes proton exchange between pyruvate and propionyl-CoA,¹³ suggesting that biotin carries protons between the active subsites. Thus, *N*¹-carboxybiotin appears to be required for generation of the substrate enolate. Critical to the validity of the enzymatic mechanism in Scheme 1 is that unimolecular CO₂ elimination be equal to or faster than the steady-state turnover rate for product formation, which is as high as 660 min⁻¹ for pyruvate carboxylase.¹⁴ In as much as the unimolecular dissociation rate for *N*-carboxyimidazolidone is reflective of that expected for *N*¹-carboxybiotin, the uncatalyzed reaction is 4 orders of magnitude too slow to be kinetically viable. Hence, an important function of the carboxyltransferase component of the carboxylase enzymes may be to catalyze the dissociation of *N*¹-carboxybiotin. Indeed, *N*¹-carboxybiotin is unstable in the carboxyl transferase subsite and is decarboxylated in a hydrolytic leak when no bound substrate is available.¹⁵ Recent measurements on the lifetime of the carboxylated 1.3S subunit of transcarboxylase give $t_{1/2} \approx 8$ h.¹⁶ This is not competitive with the steady-state reaction turnover and suggests that the hydrolytic leak is probably not the result of spontaneous decarboxylation of *N*¹-carboxybiotin before it reaches the second subsite.

We observed that the weak Lewis acid Mg²⁺ catalyzed the exchange of **2**⁻ with free CO₂, as shown by the data in Figure 6. On the basis of control experiments, this phenomenon would appear to be related to the ability of the metal ion to coordinate to **2**⁻. Given the ionic nature of the interactions between **2**⁻ and Mg²⁺ or Li⁺, it is to be expected that coordination of Mg²⁺ would be favored by its higher charge/radius ratio. This experiment was partly inspired by the previously reported observation that metal cations stabilized **2**⁻ to decarboxylation in aqueous solution.⁵ However, we find that metal ions such as Zn²⁺ result in decarboxylation of **2**⁻ in DMSO, which probably arises from its greater Brønsted acidity in the presence of trace water when compared to Mg²⁺ under similar conditions. Thus, the interaction of **2**⁻ with Mg²⁺ is more easily interpreted in the context of the uncatalyzed carboxyl exchange reaction.

The rate of carboxyl exchange exhibits a linear dependence on the concentration of the metal ion present and suggests a

reaction mechanism involving the Mg²⁺ ion interacting with **2**⁻ prior to the dissociation of CO₂, Scheme 3b. Catalysis is then achieved by the preferential stabilization of the transition state leading to Mg³⁺, which could result from the ability of the magnesium ion to relieve the buildup of negative charge on the nitrogen atom as the CO₂ dissociates. The magnesium dependent pathway would then control the rate of carboxyl exchange in the presence of Mg²⁺. Scheme 3b yields the rate law in eq 3, which assumes that magnesium binding is weak, that $2\{^{13}\text{C}\} = [\text{CO}_2]$, and that $k_f' = k_r'$.

$$\frac{d[\text{CO}_2]}{dt} = k_f'[\mathbf{2}]_0[\text{Mg}]_0K - 2k_r'K[\text{Mg}]_0[\text{CO}_2] \quad (3)$$

Equation 3 gives $k_{\text{obs}} = 2k_f'K[\text{Mg}]_0$ which is consistent with the observed linear dependence on $[\text{Mg}^{2+}]$. A value of $2k_f'K = 42(2)$ M⁻¹ min⁻¹ is obtained from the slope of the plot of $[\text{Mg}^{2+}]$ against k_{obs} . We know that Mg²⁺ binding is weak since the plot does not exhibit saturation behavior, and we are unable to calculate K from the kinetic data. Therefore, k_f' cannot be determined quantitatively, but it must be considerably greater than k_f if eq 3 is to hold. The catalytic effect of magnesium ion in nonaqueous solution contrasts with the inhibitory effect of divalent metal ions on decarboxylation of *N*-carboxyimidazolidone in aqueous solution.⁵ In the latter case, the decreased decarboxylation rates in the presence of Mn²⁺ and Cu²⁺ may be more related to their competition for protonation sites, and hence they inhibit decarboxylation by inhibiting protonation of *N*-carboxyimidazolidone.

The free acid of *N*¹-carboxybiotin is unstable to decarboxylation in aqueous solution, and this occurs at a rate substantially faster than acid-independent carboxyl exchange.⁸ Therefore, an alternative mechanism for the carboxyl transferase would involve protonation of *N*¹-carboxybiotin, followed by elimination of CO₂. This process is distinguished from Scheme 1 by the fact that proton transfer to biotin occurs prior to CO₂ elimination. This latter hypothesis is chemically viable as shown by the fact that **2**⁻ reacts with carboxylic acids to eliminate CO₂ at a rate that is more rapid than the unimolecular dissociation reaction. The overall acid-dependent decarboxylation rate in DMSO is dependent on the concentration of the acid and on its p*K*_a as shown in Figure 7. This suggests that the acid-promoted decarboxylation of **2**⁻ occurs via an acid-dependent proton-transfer preequilibrium. Fast proton transfer gives H**2**, followed by rate-limiting dissociation of CO₂, Scheme 3c. The rate law for this reaction is given in eq 4.

$$\frac{d[\text{CO}_2]}{dt} = k_2 \left[\frac{K_{\text{H}}(1+x) - \sqrt{(K_{\text{H}}(1+x) - 4(K_{\text{H}} - 1)K_{\text{H}}x)}}{2(K_{\text{H}} - 1)} \right] ([\mathbf{2}]_0 - [\text{CO}_2]) \quad (4)$$

The expression in large brackets gives the fraction of **2**⁻ in its protonated form and was derived on the basis of the proton-dependent preequilibrium for formation of H**2**, in which $x = [\text{HA}]/[\mathbf{2}]_0$. Since all of the quantities in large brackets are time-independent, eq 4 is a first-order differential equation and gives an observed first-order rate constant of

- (12) Stubbe, J.; Fish, S.; Abeles, R. H. *J. Biol. Chem.* **1980**, *255*, 236–242.
- Stubbe, J.; Abeles, R. H. *J. Biol. Chem.* **1977**, *252*, 8338–8340.
- (13) Rose, I. A.; O'Connell, E. L.; Solomon, F. J. *Biol. Chem.* **1976**, *251*, 902–904.
- (14) Legge, G. B.; Branson, J. P.; Attwood, P. V. *Biochemistry* **1996**, *35*, 3849–3856.
- (15) Wallace, J. C.; Phillips, N. B.; Snoswell, M. A.; Goodall, G. J.; Attwood, P. V.; Keech, D. B. *Ann. N.Y. Acad. Sci.* **1985**, *447*, 169–188.
- (16) Rivera-Hainaj, R. E.; Pusztaí-Carey, M.; Reddy, D. V.; Choowongkamon, K.; Sönnichsen, F. D.; Carey, P. R. *Biochemistry* **2002**, *41*, 2191–2197.

$$k_{\text{obs}} = k_2 \left[\frac{K_{\text{H}}(1+x) - \sqrt{(K_{\text{H}}(1+x) - 4(K_{\text{H}} - 1)K_{\text{H}}x)}}{2(K_{\text{H}} - 1)} \right] \quad (5)$$

Equation 5 results in saturation behavior for k_{obs} since the expression in the brackets increases from 0 to 1 as $[\text{HA}]_0$ increases. Equation 5 was fit to the data in Figure 7 to obtain a value for the terminal rate constant $k_2 = 23(2) \text{ min}^{-1}$, which is the rate constant for unimolecular elimination of CO_2 from **H2**. Assuming that this value is the same whether proton transfer occurs from acetic or benzoic acid, the slower rates for acetic acid dependent decarboxylation result from a smaller K_{H} value for acetic acid ($K_{\text{H}} = 0.022(5) \text{ M}^{-1}$) versus benzoic acid ($K_{\text{H}} = 15(4) \text{ M}^{-1}$). This is in turn consistent with the higher $\text{p}K_{\text{a}}$ for acetic acid compared with benzoic acid in DMSO.¹⁷

The CO_2 exchange experiments and the acid-dependent decarboxylation together suggest two pathways for elimination of CO_2 from **2**⁻ and, by inference, from *N*¹-carboxybiotin. An acid-independent pathway is operative in the uncatalyzed carboxyl exchange experiments and a more rapid acid-dependent pathway is operative in acid-dependent decarboxylation. The rate for elimination of CO_2 from **H2** is almost 3 orders of magnitude more rapid than from **2**⁻. This is consistent with the general stability of *N*¹-carboxybiotin and *N*-carboxyimidazolidone at neutral and higher pH and suggests that CO_2 release could then be controlled by the enzymatic system to occur only in the carboxyl transferase active site by enzyme-facilitated catalysis or proton transfer to *N*¹-carboxybiotin.

Comparing Scheme 3b and 3c, we see that the proposed mechanisms for the magnesium-catalyzed carboxyl exchange and the acid-dependent decarboxylation are chemically similar. In both cases, a Lewis acid coordinates to the carbonyl oxygen. The predicted effect is to polarize the C–N double bond away from the carboxyl group and more toward the carbonyl group. This would weaken the N– CO_2^- bond and thereby facilitate dissociation of CO_2 . Thus, Scheme 3b and 3c are similar up through the point of CO_2 dissociation. However, in Scheme 3c CO_2 dissociation is irreversible because of the very large forward driving force resulting from the tautomerization equilibrium that strongly favors the formation of **1**. While **1**[†] should be reactive toward CO_2 ,¹⁸ tautomerization (i.e., migration of the proton from O to N) competes with carboxylation, thereby preventing reentry of CO_2 . The more ionic interactions in Mg3^{3+} mean that even if migration of Mg^{2+} from O to N occurs, Mg3^{3+} remains reactive toward CO_2 . As a result, magnesium ion catalyzes reversible CO_2 dissociation instead of decarboxylation. The Mg^{2+} and acid-dependent experiments therefore show that the rate for unimolecular CO_2 exchange can be tuned by influencing specific interactions with the ureido ring, which is an important step toward understanding how CO_2 elimination might be triggered in biotin enzymes.

It has also been suggested that decarboxylation of *N*¹-carboxybiotin involves rotation of the carbamyl group out of planarity,¹⁹ which might result if the N– CO_2^- double bond character is decreased by interactions between Lewis acidic sites on the protein and the carbonyl group of *N*¹-carboxybiotin. In

simple aliphatic carbamates, C–N bond rotation has the effect of localizing the lone pair onto the nitrogen atom to a greater degree, making the nitrogen atom more nucleophilic and thus subject to protonation and decarboxylation. Indeed, such zwitterionic species are believed to be important in the acid-dependent decarboxylation of simple aliphatic carbamates.²⁰ However, the nitrogen lone pair in *N*¹-carboxybiotin is still partly delocalized into the carbonyl group even when the carboxyl group is orthogonal to the ureido ring. Thus, loss of N– CO_2 double bond character in **2**⁻ or *N*¹-carboxybiotin may not make the nitrogen appreciably more nucleophilic. This might explain why carboxyl exchange of **2**⁻ is several orders of magnitude slower than for the simple aliphatic carbamates such as lithium diethylcarbamate, which has a CO_2 exchange rate constant of at least 50 min^{-1} under the same conditions, Figure S1.²¹ The rate for CO_2 elimination from *N*¹-carboxybiotin and **2**⁻ is slowed since the nitrogen lone pair is not as available for protonation as in a simple alkylcarbamate.

Inasmuch as rapid carboxyl exchange would facilitate carboxyl transfer in the carboxylase enzymes, it is counterintuitive that the biochemical cofactor eliminates CO_2 so much more slowly than simple aliphatic carbamates, which could be biosynthesized from much simpler precursors. Indeed, at least three enzymes employ *N*-carboxylation of the amino side chain of a lysine residue to generate a carbamate group for the purpose of coordinating a metal ion.^{22–24} These carbamates are prepared from a readily available endogenous protein residue and would appear to be kinetically more reactive than *N*¹-carboxybiotin. However, the organization of the BDC enzymes into two independent active sites coupled only by *N*¹-carboxybiotin led to the hypothesis that the two subunits may have originally evolved as separate enzymes.^{2,8} In this case, a carboxyl transfer reagent would be required that was sufficiently stable to decarboxylation to freely diffuse between two isolated proteins. There would then be a chemical advantage to having a carboxyl carrier that was more stable to dissociation but whose CO_2 elimination could be triggered, for example, by interaction with a Lewis acid or by proton transfer. This stability can also serve to minimize abortive decarboxylation prior to *N*¹-carboxybiotin translocation and substrate binding. Our chemical studies lend some support to this idea by showing that unimolecular elimination of CO_2 from the *N*-carboxyimidazolidone functional group is slow but can be catalyzed by noncovalent interactions with the ureido headgroup. Indeed, a kinetic analysis of the carboxyltransferase subunit of acetyl-CoA carboxylase has identified one or more ionizable residues in the active site that

- (17) Izutsu, K. *Acid–base dissociation constants in dipolar aprotic solvents*; Blackwell Scientific Publications: Oxford, U.K., 1990.
 (18) Hegarty, A. F.; Bruce, T. C.; Benkovic, S. J. *J. Chem. Soc., Chem. Commun.* **1969**, 1173–1174.
 (19) Thatcher, G. R. J.; Poirier, R.; Kluger, R. *J. Am. Chem. Soc.* **1986**, *108*, 2699–2704.

- (20) Johnson, S. L.; Morrison, D. L. *J. Am. Chem. Soc.* **1972**, *94*, 1323–1334.
 Ewing, S. P.; Lockshon, D.; Jencks, W. P. *J. Am. Chem. Soc.* **1980**, *102*, 3072.
 (21) Deposited in Supporting Information
 (22) Rubisco: Schreuder, H. A.; Knight, S.; Curmi, P. M. G.; Andersson, I.; Cascio, D.; Sweet, R. M.; Branden, C. I.; Eisenberg, D. *Protein Sci.* **1993**, *2*, 1136–1146. Belknap, W. R.; Portis, A. R., Jr. *Biochemistry* **1986**, *25*, 1864–1869. Schreuder, H. A.; Knight, S.; Curmi, P. M. G.; Andersson, I.; Cascio, D.; Bränden, C.-I.; Eisenberg, D. *Proc. Natl. Acad. Sci. U.S.A.* **1993**, *90*, 9968–9972. Cleland, W. W.; Andrews, T. J.; Gutteridge, S.; Hartman, F. C.; Lorimer, G. H. *Chem. Rev.* **1998**, *98*, 549–561.
 (23) Urease: Park, I.-L.; Carr, M. B.; Hausinger, R. P. *Proc. Natl. Acad. Sci. U.S.A.* **1994**, *91*, 3233–3237. Park, I.-L.; Hausinger, R. P. *Science* **1995**, *267*, 1156–1158. Pearson, M. A.; Schaller, R. A.; Michel, L. O.; Karplus, P. A.; Hausinger, R. P. *Biochemistry* **1998**, *37*, 6214–6220.
 (24) Zinc-dependent phosphotriesterase: Shim, H.; Rauschel, F. M. *Biochemistry* **2000**, *39*, 7357–7364. Hong, S.-B.; Kuo, J. M.; Mullins, L. S.; Rauschel, F. M. *J. Am. Chem. Soc.* **1995**, *117*, 7580–7581.

are critical for carboxyl transfer,²⁵ suggesting that these may be part of a triggering mechanism for *N*¹-carboxybiotin dissociation.

Summary

We have presented data showing that Li $\mathbf{2}$ can undergo carboxyl exchange directly with CO₂ in DMSO. This chemical exchange reaction is suggested to occur via a unimolecular C–N bond dissociation pathway based on CO₂ exchange kinetics. The model studies suggest that unimolecular CO₂ dissociation is a viable reaction for *N*¹-carboxybiotin and that it should be considered in developing a chemical mechanism for carboxyl transfer in biotin enzymes. We observed that Mg²⁺ catalyzed the exchange of $\mathbf{2}^-$ with free CO₂, which relates to the ability of the metal ion to coordinate to $\mathbf{2}^-$. The acid-dependent decarboxylation rate of $\mathbf{2}^-$ in aprotic media is dependent on the concentration of the acid and on its p*K*_a, which suggests

that the reaction occurs via an acid-dependent proton-transfer preequilibrium. The Lewis acid catalyzed carboxyl exchange and the acid-dependent decarboxylation of *N*-carboxyimidazolone were explained within a common mechanistic framework in which C–N bond dissociation is facilitated by interaction of a cation (Mg²⁺ or H⁺) with the carbonyl group of the ureido ring. This implied that carboxyl transfer enzymes might trigger release of CO₂ from *N*¹-carboxybiotin through noncovalent interactions with the ureido ring.

Acknowledgment. Support from the National Science Foundation (CHE-9985266) is gratefully acknowledged.

Supporting Information Available: Figure S1 showing kinetic traces for CO₂ exchange by lithium diethylcarbamate. This material is available free of charge via the Internet at <http://pubs.acs.org>.

(25) Blanchard, C. Z.; Waldrop, G. L. *J. Biol. Chem.* **1998**, *273*, 19140–19145.

JA026753Y